Analytical and Bioanalytical Chemistry (2019) 411:905–913
https://doi.org/10.1007/s00216-018-1513-9

RESEARCH PAPER

An ultrasensitive signal-on electrochemiluminescence biosensor based on Au nanoclusters for detecting acetylthiocholine

Cong Zhang[1] · Yu Fan[1] · Han Zhang[1] · Shihong Chen[1] · Ruo Yuan[1]

Received: 13 October 2018 / Accepted: 22 November 2018 / Published online: 18 December 2018

Abstract

For improving the sensitivity of the electrochemiluminescent (ECL) detection and extending the applications of luminophore, the development of coreactant accelerator is one of the important ways. In this work, Au nanoclusters (Au NCs) were chosen as the luminescent material, and thiocholine, which was in situ generated by enzymatic reaction, was found to serve as a coreactant accelerator for Au NC-$S_2O_8^{2-}$ ECL system. Based on this discovery, a highly sensitive detection of acetylthiocholine (ATCl) was achieved using the acetylcholinesterase (AChE) biosensor. CeO_2 nanowires (CeO_2 NWs) were used to improve the stability of Au NCs on the glassy carbon electrode (GCE) due to the large specific surface area and good film-forming properties of CeO_2 NWs. ATCl was catalyzed by acetylcholinesterase (AChE) to produce thiocholine, which served as the coreactant accelerator to improve the ECL signal of Au NC-$S_2O_8^{2-}$ system. The biosensor obtained a low detection limit of 0.17 nM. The integration of thiocholine and Au NCs would provide a new ECL platform for bioanalysis.

Keywords Electrochemiluminescence · Biosensor · Au nanoclusters · Acetylthiocholine · Thiocholine

Introduction

Acetylthiocholine (ATCl), a synthetic substrate for acetylcholinesterase, usually plays an important role in the detection of organophosphorus pesticides and acetylcholinesterase (AChE) activity. The application of ATCl relies on the catalytic reaction of acetylcholinesterase. AChE is a serine esterase that presents in the central and nervous system of vertebrates, and it can catalyze the hydrolysis of the neurotransmitter acetylcholine in the animal's body so that the level of acetylcholine can be kept normal [1]. Similarly, ATCl can also be catalyzed by AChE to form thiocholine and acetic acid. However, the activity of AChE can be inhibited by nerve agents, such as organophosphorus pesticides, carbamates, and pyrethroids, which have high toxicity for AChE. The inhibition of AChE activity will cause the concentration of acetylcholine higher than normal levels, thus leading to fibrillation, arrhythmia, and other serious illnesses [2–5]. Based on the above principles, the AChE sensor is a commonly used technique for detecting nerve inhibitors or AChE activity owning to its rapid response, high sensitivity, and selectivity. The enzymatic reactions involved in the AChE-based sensor system are as follows:

$$\text{Acetylthiocholine} + H_2O \xrightarrow{\text{AChE}} \text{Thiocholine} + \text{Acetate} \quad (1)$$

$$\text{Thiocholine} + O_2 \xrightarrow{\text{ChO}} \text{BetaineAdehyde} + H_2O_2 \quad (2)$$

ATCl is hydrolyzed to acetic acid and thiocholine by AChE. Thiocholine is further oxidized by choline oxidase (ChO) in the presence of oxygen to produce H_2O_2. Based on the reactant (dissolved O_2) and the product (thiocholine, acetate or H_2O_2) in above enzymatic reactions, a series of AChE-based methods have been established for the quantitative determination of organophosphorus, including electrochemical and ECL sensors, colorimetric, fluorescence, and photoluminescence methods [6–10]. Since the establishment of the above method would depend on the presence of enzyme substrate ATCl, the detection of ATCl is of great significance.

Recently, ECL technique received special attention due to its unique advantages, such as wide dynamic range, high sensitivity, low background signal, and simple instrumentation [11]. Various types of ECL luminophores, including

✉ Shihong Chen
cshong@swu.edu.cn

[1] Key Laboratory of Luminescent and Real-Time Analytical Chemistry, Ministry of Education, College of Chemistry and Chemical Engineering, Southwest University, Chongqing 400715, China

$Ru(bpy)_3^{2+}$, semiconductor nanocrystals (or quantum dots), luminol, perylene and its derivatives, graphite-like carbon nitride (g-C_3N_4), polymer dots (PDs), and so forth, have been reported [12]. However, the shortcomings of these luminophores cannot be ignored. For instance, most of the quantum dots were synthetized using heavy metal ions and their toxicity limits their application. Polymer dots generally involve toxic solvents in the synthesis process. The application of perylene and its derivatives is also limited due to their poor water solubility. So it is important to exploit non-toxic and environmentally friendly luminescent materials.

Metal nanoclusters (e.g., Pt, Au, Ag, Cu) have been gradually applied in molecular recognition, biomedical research, and chemical and biologic sensing. The low toxicity, ease of synthesis, and good biocompatibility of metal nanoclusters make them alternative ECL luminescent materials. Especially, the discrete electronic energy levels and molecule-like properties of Au nanoclusters (Au NCs) endow them excellent electrochemical, catalytic, and optical properties [13–16]; thus, many researchers are dedicated to Au NC-based ECL sensor. For example, Zhu's group reported the cathodic ECL behavior of Au NCs with $S_2O_8^{2-}$ as coreactant and achieved the detection of dopamine [17]. Wu et al. constructed an ECL biosensor using Au NCs as ECL emitter and $K_2S_2O_8$ as coreactant for the detection of CEA [18]. Our group fabricated a biosensor based on the quenching effect of ferrocenecarboxylic acid to Au NC-triethylamine ECL system for detecting concanavalin A [19]. Presently, researchers commonly utilized the coreagent such as $S_2O_8^{2-}$, tripropylamine, or H_2O_2 to amplify the ECL luminous intensity of Au NCs. In order to expand the application of Au nanocluster ECL system, it is necessary to explore more coreagent or coreactant accelerator of Au NC ECL system.

Cerium is a rare earth element, and its oxide has been widely researched in catalysis, solar and fuel cells, oxygen sensing, and ultraviolet absorbance owning to its oxygen storage capacity, high mechanical strength, biocompatibility, nontoxicity, and large specific surface area [20–23]. The application of CeO_2 in ECL sensors was mainly attributed to the high electron transfer efficiency of CeO_2 with Ce^{4+}/Ce^{3+} redox pair, which could further improve the performance of the biosensor [24, 25].

In this work, the composites of CeO_2 nanowires (CeO_2 NWs) and Au NCs were prepared and used as matrix for immobilizing AChE to construct an AChE-based biosensor. AChE catalyzed the hydrolysis of ATCl to generate thiocholine, which served as the coreactant accelerator of Au NCs-$S_2O_8^{2-}$ system to improve the ECL signal, thus achieving the detection of ATCl. CeO_2 NWs with a large specific surface area and good film-forming ability can improve the stability of Au NCs and achieve the high loading of Au NCs on the electrode. Also, the high electron transfer efficiency of CeO_2 NWs could improve the sensitivity of the detection. The investigation of thiocholine as a coreactant accelerator of Au NCs-$S_2O_8^{2-}$ system would extend the application of Au NCs and add some new insight to AChE-based ECL-sensing platform.

Experimental

Reagents and chemicals

Acetylcholinesterase (AChE, type C2888-1KU), acetylthiocholine (ATCl), bovine serum albumin (BSA), and gold chloride tetrahydrate ($HAuCl_4 \cdot 4H_2O$) were obtained from Sigma Chemical Co. (St. Louis, MO, USA). Potassium persulfate ($K_2S_2O_8$), NaOH, $CeCl_3 \cdot 7H_2O$, and NaCl were acquired from Chengdu Kelong Chemical Industry (Chengdu, China). Human serum samples of volunteers were provided by the 9th People's Hospital of Chongqing. The 9th People's Hospital of Chongqing Committee approved our studies, and all volunteers gave informed consent. The stock solution of 0.10 M KH_2PO_4 and K_2HPO_4 was used to prepare phosphate buffer solutions (PBS) with various pH values.

Apparatus

A MPI-E electrochemiluminescence analyzer (Xi'an Remax Electronic Science & Technology Co. Ltd., China) was used for the ECL detection. A CHI 600D electrochemical work station (Shanghai CH Instruments, China) was used for cyclic voltammetry (CV) detection. During the ECL detection, the voltage of 800 V was set at the photomultiplier tube (PMT) and the potential scan of − 1.5~0 V was adopted. A modified glassy carbon electrode and platinum wire were used as the working electrode and auxiliary, respectively. And a saturated calomel electrode (SCE) or Ag/AgCl (sat. KCl) was used as reference electrode. UV-2450 UV-vis spectrophotometer (Shimadzu, Japan) and F-4500 spectrofluorophotometer (Hitachi, Japan) were used to record UV–visible (UV–vis) absorption spectra and fluorescence spectrometry, respectively. The morphologies of nanocomposites were analyzed by a scanning electron microscopy (SEM, S-4800, Hitachi, Japan).

Preparation of CeO_2 NWs

CeO_2 NWs were prepared by hydrothermal and calcination method [26]. 0.523 g NaCl, 3.6 g NaOH, and 279 mg $CeCl_3 \cdot 7H_2O$ were dissolved in 15 mL deionized water together. The resulting soliquoid was transferred to a 25-mL steel autoclave and heated to 180 °C for 24 h. The white solid product was centrifuged at 8000 rpm for 5 min and washed three times with deionized water. Subsequently, the product was dried at 200 °C for 12 h. CeO_2 NWs were obtained by heating the product at 600 °C for 3 h (ramping rate

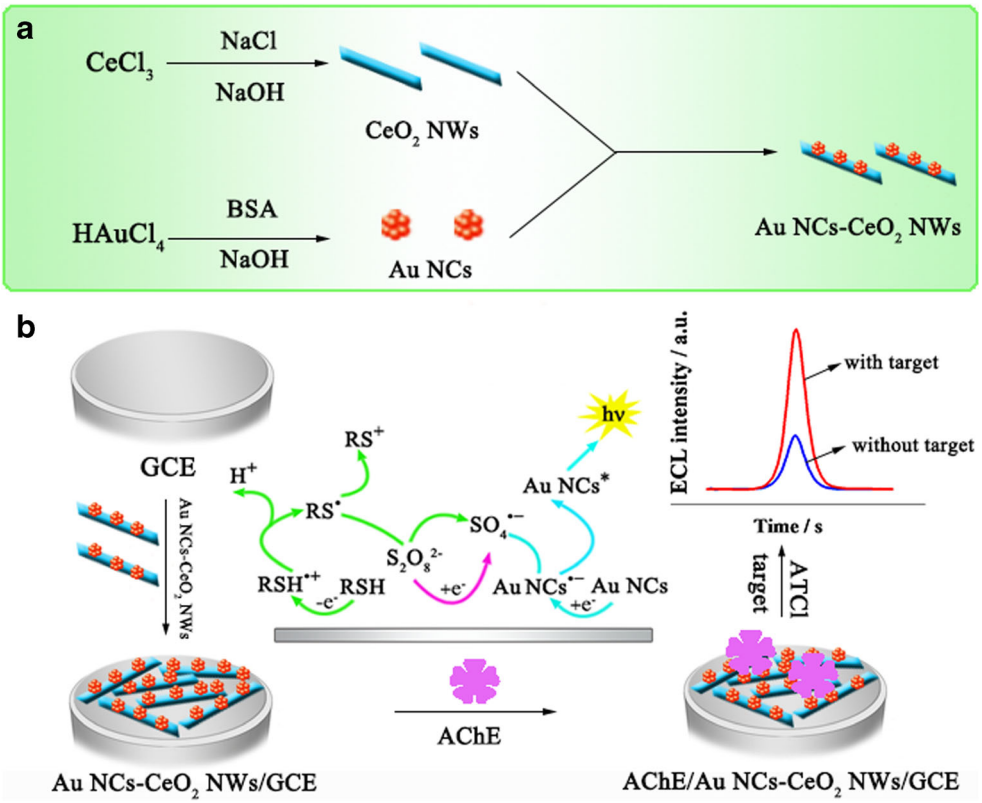

Scheme 1 **A** Preparation procedure of Au NC-CeO_2 NW composite. **B** Fabrication process of the biosensor and the possible luminescence mechanism

10 °C min^{-1}) and then cooled to room temperature. CeO_2 NWs were dispersed in deionized water for further use.

Preparation of Au NCs

The Au NCs were obtained by a simple one-step reaction [27]. Five milliliters of 10 mM $HAuCl_4$ solution (37 °C) was added to 5 mL of 50 mg/mL BSA solution (37 °C). After stirring vigorously for 2 min, 0.5 mL of 1.0 M NaOH solution (37 °C) was added into the mixture. During the mixture was stirred at 37 °C for 12 h, the starting yellow solution gradually turns brown. Finally, the prepared Au NC solution was dialyzed in deionized water for 48 h to make it purer. The Au NC solution was stored in a refrigerator for further use. During the preparation of Au NCs, the protein molecule BSA sequestered Au ions and entrapped them. After the pH of the solution was adjusted to ~12, the reducing ability of BSA was activated and the captured Au ions were reduced in situ to Au NCs [27]. Here, BSA acts as both a template support and a reducing agent in the synthesis of Au NCs.

Preparation of Au NC-CeO_2

The Au NC-CeO_2 NWs was prepared by mixing CeO_2 NW dispersion liquid and Au NC solution by ultrasound. Firstly, 0.75 mg of CeO_2 NWs was dispersed into 1 mL deionized water. Subsequently, 2.5 mL of Au NCs solution was added into and further mixed by ultrasound. The resulted Au NC-CeO_2 NWs composite was stored at 4 °C for further use. The preparation procedure of Au NC-CeO_2 NW composite was shown in Scheme 1A.

Fabrication of the biosensor

The preparation process of the biosensor is illustrated in Scheme 1. After polished with 0.3 μm and 50 nm alumina slurry, respectively, the glassy carbon electrode (GCE) was washed ultrasonically with deionized water and anhydrous ethanol. The as-prepared Au NC-CeO_2 NWs (20 μL) was dropped onto the cleaned GCE and desiccated in air. Then, 10 μL of AChE solution (250 u/mL), prepared with 0.10 M pH 7.4 PBS, was dropped onto the electrode surface and dried in refrigerator. The ECL response of the designed biosensor was detected in the presence of 0.10 M $K_2S_2O_8$ as coreactant.

Results and discussion

Characterization of the synthesized nanomaterials

SEM and TEM were employed to examine the morphologies and microstructures of the nanomaterials. Figure 1A displays the TEM image of Au NCs with the diameter of below 2.5 nm, and the size distributed homogeneously. Figure 1B presents

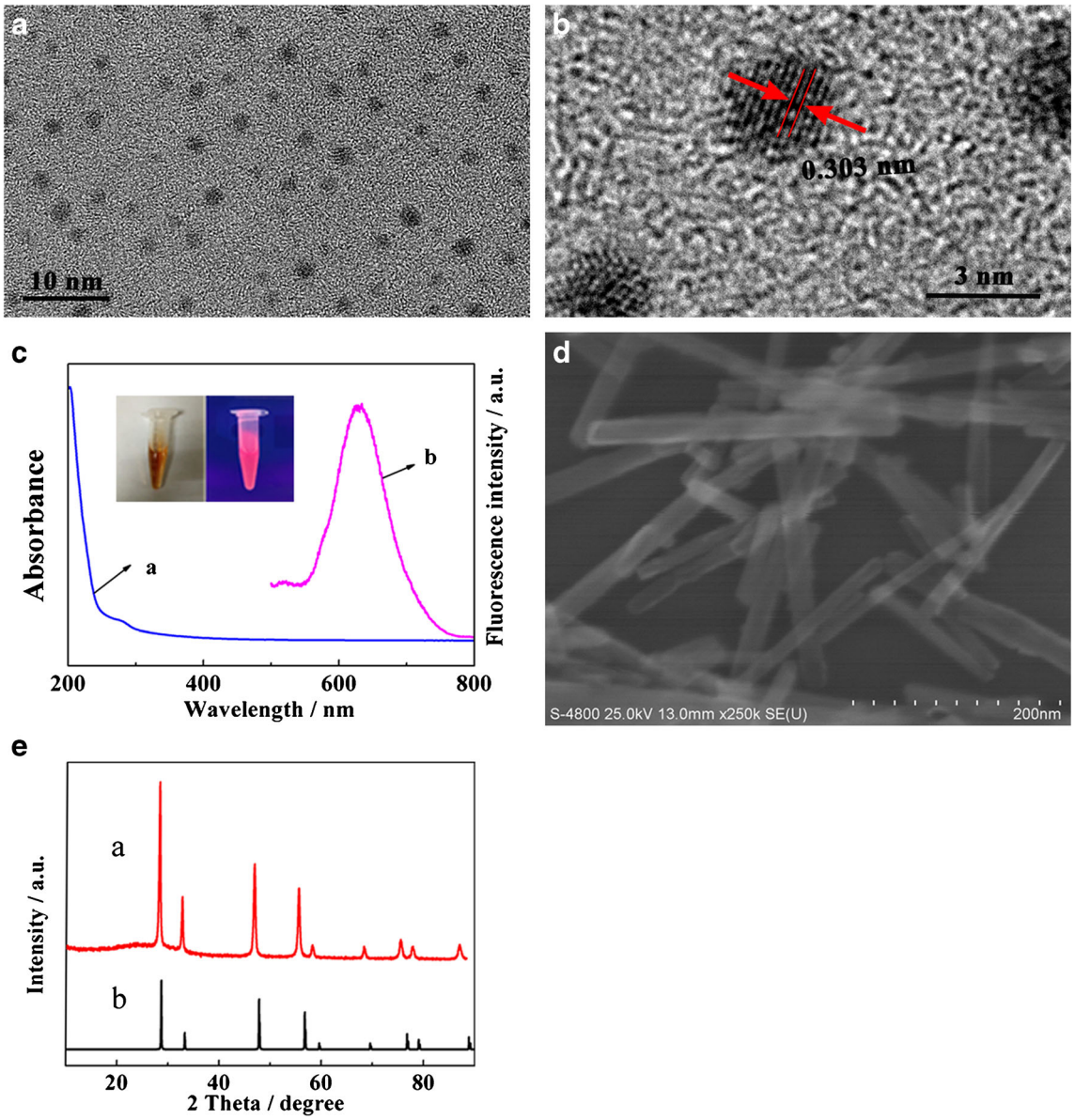

Fig. 1 **A** TEM and **B** high-resolution TEM image of Au NCs. **C** (a) UV–vis absorption and (b) fluorescence (excitation at 470 nm) spectra of Au NCs. The inset of **C**: photograph of Au NC solution under room light and UV light irradiation. **D** SEM image of CeO_2 NWs. **E** The XRD pattern of the prepared CeO_2 (a) and standard card for CeO_2 (b)

the high-resolution TEM image of Au NCs and the crystal lattice structure with the interplanar spacing of about 0.303 nm can be observed. Additionally, UV–vis absorption and fluorescence emission of Au NCs were also explored. Figure 1C curve a shows the UV–vis absorption spectra of Au NCs. The absorption peak at 275 nm was observed, which was resulted from the amino acid residues of BSA [27]. The fluorescence emission spectroscopy of as-synthesized Au NCs is shown in Fig. 1C curve b, and maximum emission wavelength at 630 nm was observed, which was consistent with previous report [28]. The inset of Fig. 1C exhibits the strong red fluorescence under UV light and brown color under visible light of Au NC solution. The microstructure of CeO_2 NWs was directly confirmed by SEM and the result is shown in Fig. 1D. As seen, wire-like CeO_2 was formed and the width was about 20–30 nm, which was consistent with the literature [26]. The XRD test was performed on the prepared CeO_2 and the test results were compared with the XRD standard card of CeO_2. As shown in Fig. 1E, the diffraction pattern of the product (curve a) has nine peaks at 28.7°, 33.3°, 47.8°, 57°, 59.8°, 69.8°, 76.8°, 79.3°, and 88.9°, respectively, which are consistent with the characteristic peaks of CeO_2 (JCPDS card No. 1–800) (curve b). The above results indicate that CeO_2 was successfully prepared.

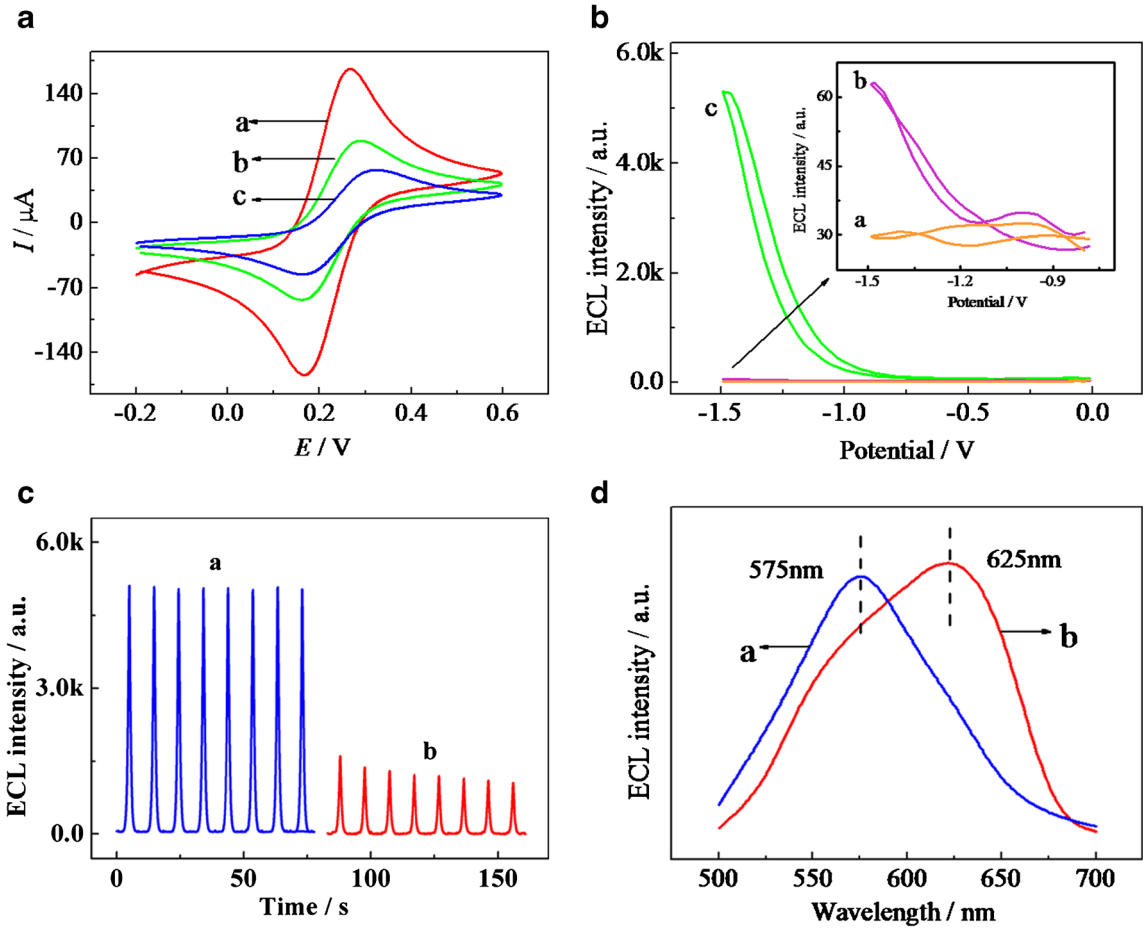

Fig. 2 **A** CV waves in 5.0 mM $K_3[Fe(CN)_6]/K_4[Fe(CN)_6]$ at (a) bare GCE, (b) Au NCs-CeO_2 NWs/GCE, and (c) AChE/Au NCs-CeO_2 NWs/GCE. **B** ECL curves at (a) CeO_2 NWs/GCE, (b) Au NCs/GCE in 0.10 M pH 7.4 PBS without coreactant, and (c) Au NCs-CeO_2 NWs/GCE in 0.10 M pH 7.4 PBS containing 0.10 M $S_2O_8^{2-}$. **C** The ECL response of Au NCs-CeO_2 NWs (a) and Au NCs (b) modified GCE with continuously cyclic potential scanning for 8 cycles in 0.10 M PBS (pH 7.4) containing 0.10 M $S_2O_8^{2-}$. **D** ECL spectra of typical $S_2O_8^{2-}/O_2$ system (curve a) and Au NCs-$S_2O_8^{2-}$ (curve b)

CV characterization of the biosensor

CV was used to characterize the stepwise modification of the biosensor in 5 mM $[Fe(CN)_6]^{4-/3-}$ solution with a scan rate of 50 mV/s. As shown in Fig. 2A, a well-defined CV curve of ferricyanide ions was observed at bare GCE (curve a). When Au NC-CeO_2 NWs was modified onto the GCE, the redox peak currents decreased (curve b) due to the template BSA of Au NCs, which hampered the electron transfer. When AChE was loaded on the Au NC-CeO_2 NW-modified electrode surface, the redox peak currents further decreased (curve c) owing to the low conductivity of AChE. This result demonstrated the successful assembly of the biosensor.

ECL response of differently modified electrodes and possible ECL mechanisms

The ECL properties of Au NCs and CeO_2 NWs were investigated in 0.10 M pH 7.4 PBS without coreactant. As shown in Fig. 2B, CeO_2 NW-modified GCE had no obvious luminescence (curve a) and Au NC-modified GCE exhibited a weak luminous intensity (curve b) at −1.5 V, suggesting that AuNCs has a certain luminous performance but CeO_2 NWs did not. For Au NC-CeO_2 NW-modified electrode, a high ECL intensity was acquired in the presence of 0.10 M $S_2O_8^{2-}$ (curve c), which was mainly attributed to the following two reasons. Firstly, the large specific surface area and good membrane film-forming property of CeO_2 NWs were beneficial to the high loading of Au NCs on the electrode. Secondly, $S_2O_8^{2-}$ served as the coreactant to enhance the luminescence of Au NCs. Additionally, in order to confirm that CeO_2 NWs can improve the stability of the Au NCs as well as the ECL stability, continuously cyclic potential scanning was performed at the electrode modified with Au NC-CeO_2 NWs and Au NCs, respectively. As shown in Fig. 2C, with continuously cyclic potential scanning for 8 cycles in 0.10 M PBS (pH 7.4) containing 0.10 M

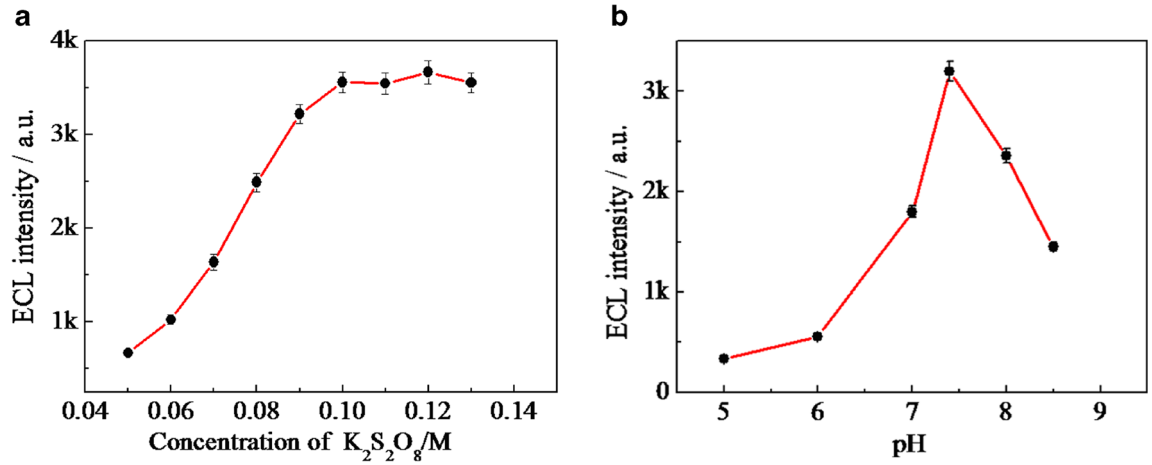

Fig. 3 Effect of **A** the concentration of $K_2S_2O_8$ on the ECL responses in pH 7.4 PBS and **B** pH of PBS on the ECL responses in the presence of 0.10 M $K_2S_2O_8$

$S_2O_8^{2-}$, Au NC-CeO_2 NW-modified GCE exhibits a more stable and higher ECL signal than Au NC-modified electrode without CeO_2 NWs. The relative standard deviations (RSD) of ECL intensity for 8-cycle scanning were 0.7% and 14.7%, respectively, indicating that CeO_2 NWs was beneficial to improve the stability of the Au NCs as well as the ECL stability.

To explore the influence of $S_2O_8^{2-}$ on the luminescence of Au NCs, the ECL spectra of typical $S_2O_8^{2-}/O_2$ and Au NCs-$S_2O_8^{2-}$ system were measured using optical filter, respectively. As shown in Fig. 2D, the ECL emission peak of $S_2O_8^{2-}/O_2$ in the absence of Au NCs was observed at 575 nm (curve a). However, the ECL emission peak of Au NCs-$S_2O_8^{2-}$ was observed at 625 nm (curve b), which was obviously different from the characteristic peak of $S_2O_8^{2-}/O_2$ (575 nm) without Au NCs. Furthermore, the ECL emission peak of Au NCs-$S_2O_8^{2-}$ was close to the PL emission spectrum of 630 nm for Au NCs. Above fact proved that the ECL luminophore was AuNCs rather than $S_2O_8^{2-}/O_2$.

According previous reports [6, 29], the possible ECL mechanisms are presented as follows:

$$\text{Au NCs} + e^- \rightarrow \text{Au NCs}^{\bullet -}$$

$$S_2O_8^{2-} + e^- \rightarrow S_2O_8^{\bullet 2-}$$

$$S_2O_8^{\bullet 2-} \rightarrow SO_4^{2-} + SO_4^{\bullet -}$$

$$RSH - e^- \rightarrow RSH^{\bullet +}$$

$$RSH^{\bullet +} - H^+ \rightarrow RS^{\bullet}$$

$$S_2O_8^{2-} + RS^{\bullet} \rightarrow RS^+ + SO_4^{2-} + SO_4^{\bullet -}$$

$$\text{Au NCs}^{\bullet -} + SO_4^{\bullet -} \rightarrow \text{Au NCs}^* + SO_4^{2-}$$

$$\text{Au NCs}^* \rightarrow \text{Au NCs} + h\nu$$

Firstly, $S_2O_8^{2-}$ was reduced to $SO_4^{\bullet -}$, a substance with strong oxidizability. Produced thiocholine (RSH) under the catalysis of AChE can be oxidized to $RS^{\bullet}$. Meanwhile, $RS^{\bullet}$ and $S_2O_8^{2-}$ interacted to generate $SO_4^{\bullet -}$, thus resulting in an increase of the amount of $SO_4^{\bullet -}$. $SO_4^{\bullet -}$ and Au $NCs^{\bullet -}$

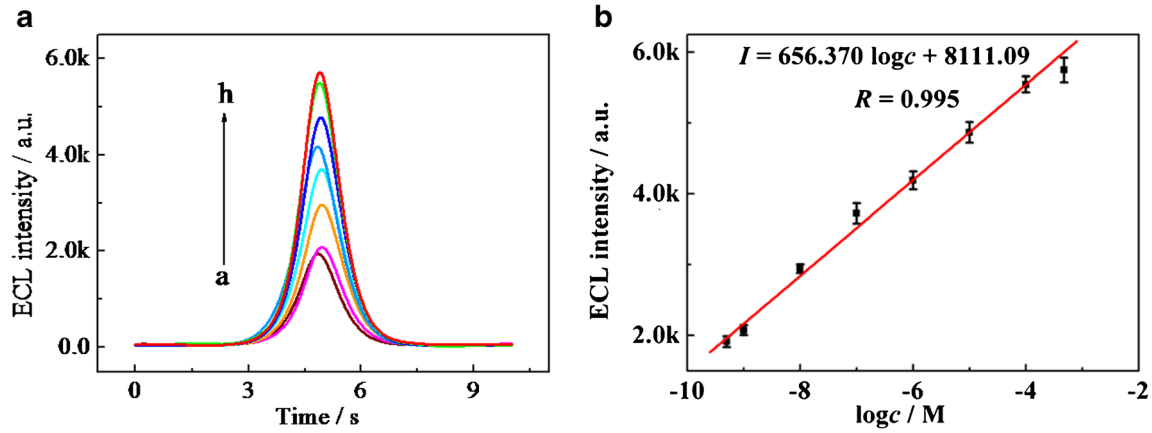

Fig. 4 **A** ECL responses of the biosensor in 0.10 M PBS (pH 7.4) containing $S_2O_8^{2-}$ (0.10 M) and ATCl with different concentrations: (a) 0.50 nM; (b) 1.0 nM; (c) 10 nM; (d) 100 nM; (e) 1.0 μM; (f) 10 μM; (g) 100 μM; and (h) 0.47 mM. **B** The linear calibration curve

Table 1 Comparison of reported methods for ATCl determination

Method	Linear range (mM)	Detection limit (mM)	Reference
Amperometry	2.0×10^{-3}–4.0×10^{-1}	0.10×10^{-3}	[31]
Amperometry	0.10–1.5	5.0×10^{-2}	[32]
Amperometry	9.9×10^{-3}–2.03	–	[33]
Electrochemiluminescence	6.7×10^{-6}–9.2×10^{-1}	2.2×10^{-6}	[5]
Electrochemiluminescence	5.0×10^{-7}–4.7×10^{-1}	1.7×10^{-7}	This work

generated by the electron exchange on the GCE surface can interact to generate Au NCs*, which acts as light-emitting species and achieves the detection of ATCl.

Optimization of experimental conditions

In order to obtain the optimal experimental conditions, the effect of pH of PBS and concentration of $K_2S_2O_8$ on the performance of biosensor was investigated. As shown in Fig. 3A, the ECL signals obviously increased with increasing $S_2O_8^{2-}$ concentrations from 0.050 to 0.10 M, which was due to the fact that $S_2O_8^{2-}$ was reduced to $SO_4^{\bullet-}$ and $SO_4^{\bullet-}$ can interact with Au NCs$^{\bullet-}$ to generate Au NCs*. With the increase in $S_2O_8^{2-}$ concentration, the produced $SO_4^{\bullet-}$ increased, followed by generating more Au NCs*; thus, the ECL signal increased. When the concentration of $S_2O_8^{2-}$ was higher than 0.10 M, the ECL intensity changed slightly and reached relatively stable value. The reasonable explanation may be as follows. The excited state of Au NCs* would react with excessive $S_2O_8^{2-}$, which would consume the Au NCs*, thus inhibiting the further increasing of ECL intensity. Similar quenching reaction was observed between carbon quantum dots (C*) and Au NCs* [30]. Therefore, 0.10 M was used as the optimum concentration in the detection process.

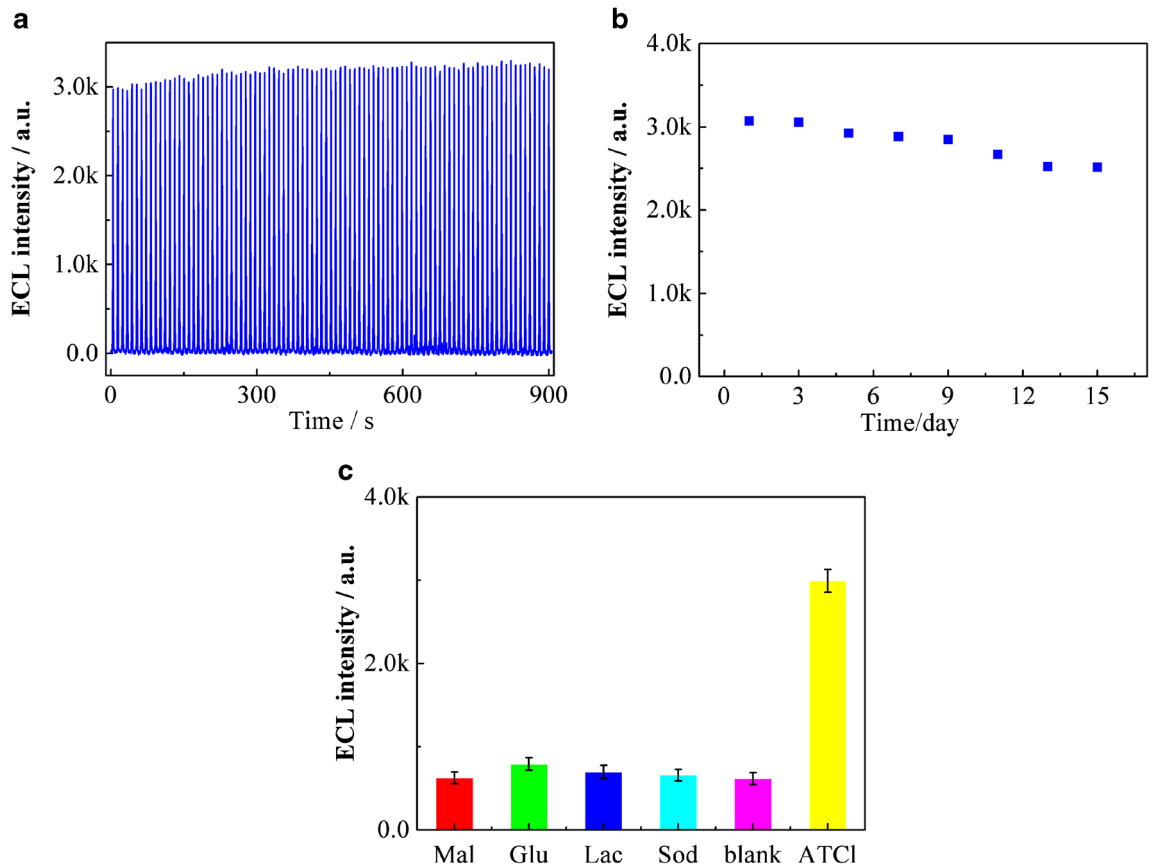

Fig. 5 **A** The ECL stability of the biosensor with continuously cyclic potential scanning for 100 cycles containing 10 nM ATCl. **B** Time-dependent stability of the proposed biosensor towards 10 nM ATCl. **C** Selectivity of the biosensor for the detection of ATCl (10 nM) against 0.30 mM maltose, glucose, lactose, and sodium nitrite. The ECL signals were measured in 0.10 M PBS (pH 7.4) containing 0.10 M $S_2O_8^{2-}$

Table 2 Recoveries of ATCl by the biosensor in human serum

Samples	Added (mM)	Found[a] (mM)	Recovery (%)
1	0.100	0.098 ± 0.005	102
2	0.200	0.195 ± 0.005	99.5
3	0.300	0.298 ± 0.015	95.3

[a] Average of three determination ± SD, $n = 3$

The effect of pH of PBS on the biosensor performance was investigated. As shown in Fig. 3B, the maximum ECL intensity was obtained at pH 7.4. The solution always contained 100 nM ATCl during the optimization experiment.

Performance of the biosensor

Calibration curve

The proposed ECL biosensor for determining ATCl was explored under the optimum conditions. The ECL intensity of the prepared biosensor increased with increasing the concentration of ATCl and a good linear relationship between the ECL intensity and the logarithm of concentration of ATCl was achieved (Fig. 4). The linear range was from 0.50 nM to 0.47 mM with a detection limit of 0.17 nM. The linear regression equation was $I = 656.370\log c + 8111.09$, and the correlation coefficient of $R = 0.995$. As shown in Table 1, compared to previous reports, the biosensor prepared in this work exhibited a lower detection limit and a wider linear range.

Stability of the biosensor

To investigate the operational stability of the biosensor, the ECL signals of the biosensor with continuously cyclic potential scanning for 100 cycles were investigated, and the result was shown in Fig. 5A. As expectedly, the biosensor exhibited a good stability under continuous cyclic scanning. In addition, the time-dependent stability of ECL biosensors was tested. The ECL response of the biosensor towards 10 nM ATCl was tested every 2 days. As shown in Fig. 5B, after 15 days, the ECL intensity decreased 18.1%, demonstrating an acceptable time-dependent stability of the ECL biosensor.

Selectivity of the biosensor

The selectivity is an important evaluation criterion for a biosensor. The selectivity of our proposed biosensor was investigated using maltose (Mal), sodium nitrite (SN), lactose (Lac), and glucose (Glu) as the interfering substances. As shown in Fig. 5C, the interfering substances with 30-fold concentration of ATCl (10 nM) did not cause a significant interference for the prepared biosensor. This result indicated a good anti-interference capability of the biosensor.

Application of the biosensor

The practicability of the biosensor was studied in human serum using standard addition methods. As shown in Table 2, the recoveries ranged between 95.3 and 102%, indicating that the prepared biosensor is practical in the actual detection of ATCl.

Conclusions

In this paper, the thiocholine as the coreactant accelerator of ECL system was reported for the first time. Based on the fact that thiocholine produced in the AChE-based enzymatic reactions would enhance the ECL signal of Au NCs-$S_2O_8^{2-}$ system, the sensitive detection of ATCl was achieved. CeO_2 NWs exhibits large specific surface area, good film-forming properties, and high electron transfer efficiency, and its introduction would achieve the high loading of Au NCs on the electrode, thus improving the sensitivity of the detection. The integration of thiocholine and Au NCs would provide a promising ECL platform for AChE bioanalysis.

Funding information This work was supported by National Natural Science Foundation of China (21775122, 21775123, 51473136, 21575116) and Nature Science Foundation of Chongqing City (cstc2018jcyjAX0693) China.

Compliance with ethical standards

Informed consent The 9th People's Hospital of Chongqing Committee approved our studies, and all volunteers gave informed consent.

Conflict of interest The authors declare that they have no conflict interest.

Publisher's note Springer Nature remains neutral with regard to jurisdictional claims in published maps and institutional affiliations.

References

1. Mileson BE, Chambers JE, Chen WL, Dettbarn W, Ehrich M, Eldefrawi AT, et al. Common mechanism of toxicity: a case study of organophosphorus pesticides. Toxicol Sci. 1998;41:8–20.
2. Zhang SX, Xue SF, Deng JJ, Zhang M, Shi GY, Zhou TS. Polyacrylic acid-coated cerium oxide nanoparticles: an oxidase mimic applied for colorimetric assay to organophosphorus pesticides. Biosens Bioelectron. 2016;85:457–63.
3. Wang CI, Chen WT, Chang HT. Enzyme mimics of Au/Ag nanoparticles for fluorescent detection of acetylcholine. Anal Chem. 2012;84:9706–12.
4. Liao SZ, Han WT, Ding HZ, Xie DX, Tan H, Yang SY, et al. Modulated dye retention for the signal-on fluorometric

determination of acetylcholinesterase inhibitor. Anal Chem. 2013;85:4968–73.
5. Wu XP, Zhong X, Chai YQ, Yuan R. Electrochemiluminescence acetylcholine biosensor based on biofunctional AMs-AChE-ChO biocomposite and electrodeposited graphene-Au-chitosan nanocomposite. Electrochim Acta. 2014;147:735–42.
6. Liu GD, Lin YH. Biosensor based on self-assembling acetylcholinesterase on carbon nanotubes for flow injection/amperometric detection of organophosphate pesticides and nerve agents. Anal Chem. 2006;78:835–43.
7. Qian SH, Lin HW. Colorimetric sensor array for detection and identification of organophosphorus and carbamate pesticides. Anal Chem. 2015;87:5395–400.
8. Meng XW, Wei JF, Ren XL, Ren J, Tang FL. A simple and sensitive fluorescence biosensor for detection of organophosphorus pesticides using H_2O_2-sensitive quantum dots/bi-enzyme. Biosens Bioelectron. 2013;47:402–7.
9. Yi YH, Zhu GB, Liu C, Huang Y, Zhang YY, Li HT, et al. A label-free silicon quantum dots-based photoluminescence sensor for ultrasensitive detection of pesticides. Anal Chem. 2013;85:11464–70.
10. Chen HM, Zhang H, Yuan R, Chen SH. Novel double-potential electrochemiluminescence ratiometric strategy in enzyme-based inhibition biosensing for sensitive detection of organophosphorus pesticides. Anal Chem. 2017;89:2823–9.
11. Richter M. Electrochemiluminescence (ECL). Chem Rev. 2004;104:3003–36.
12. Li LL, Chen Y, Zhu JJ. Recent advances in electrochemiluminescence analysis. Anal Chem. 2017;89:358–71.
13. Tian R, Zhang ST, Li MW, Zhou YQ, Lu B, Yan DP, et al. Localization of Au nanoclusters on layered double hydroxides nanosheets: confinement-induced emission enhancement and temperature-responsive luminescence. Adv Funct Mater. 2015;25:5006–15.
14. Tao Y, Li MQ, Ren JS, Qu XG. Metal nanoclusters: novel probes for diagnostic and therapeutic applications. Chem Soc Rev. 2015;44:8636–63.
15. Zhao M, Chen AY, Huang D, Zhuo Y, Chai YQ, Yuan R. Cu nanoclusters: novel electrochemiluminescence emitters for bioanalysis. Anal Chem. 2016;88:11527–32.
16. Hesari M, Workentin MS, Ding ZF. Highly efficient electrogenerated chemiluminescence of Au_{38} nanoclusters. ACSNANO. 2014;8:8543–53.
17. Li LL, Liu HY, Shen YY, Zhang JR, Zhu JJ. Electrogenerated chemiluminescence of Au nanoclusters for the detection of dopamine. Anal Chem. 2011;83:661–5.
18. Lv XH, Ma HM, Wu D, Yan T, Ji L, Liu YX, et al. Novel gold nanocluster electrochemiluminescence immunosensors based on nanoporous NiGd–Ni_2O_3–Gd_2O_3 alloys. Biosens Bioelectron. 2016;75:142–7.
19. Chen SH, Fan Y, Zhang C, He YY, Wei SP. Quenched solid-state electrochemiluminescence of gold nanoclusters and the application in the ultrasensitive detection of concanavalin A. Electrochim Acta. 2017;228:195–202.
20. Hussain S, Al-Nsour F, Rice AB, Marshburn J, Yingling B, Ji ZX, et al. Cerium dioxide nanoparticles induce apoptosis and autophagy in human peripheral blood monocytes. ACSNANO. 2012;6(7):5820–9.
21. Kaushik A, Solanki PR, Pandey MK, Ahmad S, Malhotra BD. Cerium oxide-chitosan based nanobiocomposite for food borne mycotoxin detection. Appl Phys Lett. 2009;95:173703.
22. Hammond OS, Edler KJ, Bowron DT, Torrente-Murciano L. Deep eutectic-solvothermal synthesis of nanostructured ceria. Nature Com. 2016;8:14150.
23. Tana ZML, Li J, Li HJ, Li Y, Shen WJ. Morphology-dependent redox and catalytic properties of CeO_2 nanostructures: nanowires, nanorods and nanoparticles. Catal Today. 2009;148:179–83.
24. Zhou Y, Chen MX, Zhuo Y, Chai YQ, Xu WJ, Yuan R. In situ electrodeposited synthesis of electrochemiluminescent Ag nanoclusters as signal probe for ultrasensitive detection of cyclinD1 from cancer cells. Anal Chem. 2017;89:6787–93.
25. Wang JX, Zhuo Y, Zhou Y, Wang HJ, Yuan R, Chai YQ. Ceria doped zinc oxide nanoflowers enhanced luminol-based electrochemiluminescence immunosensor for amyloid-β detection. ACS Appl Mater Interfaces. 2016;8:12968–75.
26. Ke J, Zhu W, Jiang YY, Si R, Wang YJ, Li SC, et al. Strong local coordination structure effects on subnanometer PtOx clusters over CeO_2 nanowires probed by low-temperature CO oxidation. ACS Cata. 2015;5:5164–73.
27. Xie JP, Zheng YG, Ying JY. Protein-directed synthesis of highly fluorescent gold nanoclusters. J Am Chem Soc. 2009;131:888–9.
28. Shu T, Wang JX, Su L, Zhang XJ. Chemical etching of bovine serum albumin-protected Au_{25} nanoclusters for label-free and separation-free ratiometric fluorescent detection of tris(2-carboxyethyl)phosphine. Anal Chem. 2016;88:11193–8.
29. Ma MN, Zhuo Y, Yuan R, Chai YQ. New signal amplification strategy using semicarbazide as coreaction accelerator for highly sensitive electrochemiluminescent aptasensor construction. Anal Chem. 2015;87:11389–97.
30. Li JZ, Wang NY, Tran TT, Huang CA, Chen L, Yuan LJ, et al. Electrogenerated chemiluminescence detection of trace level pentachlorophenol using carbon quantum dots. Analyst. 2013;138:2038–43.
31. Du D, Huang X, Cai J, Zhang AD, Ding JW, Chen SZ. An amperometric acetylthiocholine sensor based on immobilization of acetylcholinesterase on a multiwall carbon nanotube–cross-linked chitosan composite. Anal Bioanal Chem. 2007;387(3):1059–65.
32. Cumpu MB, Nesakumar N, Nagarajan S, Ramanujam S, Krishnan UM, Babu KJ, et al. Design and development of acetylthiocholine electrochemical biosensor based on zinc oxide–cerium oxide nanohybrid modified platinum electrode. Bull Environ Contam. 2017;98:662–71.
33. Yang YH, Guo MM, Yang MH, Wang ZJ, Shen GL, Yu RQ. Determination of pesticides in vegetable samples using an acetylcholinesterase biosensor based on nanoparticles ZrO_2/chitosan composite film. Int J Environ Anal Chem. 2005;85:163–75.